MAUSAM, **75**, 4 (October 2024), 977-992

MAUSAM

DOI : https://doi.org/10.54302/mausam.v75i4.6624
Homepage: https://mausamjournal.imd.gov.in/index.php/MAUSAM

UDC No. 358.551.50892:004.383.8

Prediction of Low-Visibility Events by Integrating the Potential of Persistence and Machine Learning for Aviation Services

ANAND SHANKAR[*,#*], BIKASH CHANDRA SAHANA* and SURENDRA PRATAP SINGH[**]

**Department of Electronics & Communication Engineering,*

National Institute of Technology, Patna, Bihar - 800 005, India

*#*Ministry of Earth Sciences, Govt. of India, Patna, Bihar - 800 002, India*

***Ministry of Earth Sciences, Govt. of India, New Delhi, Delhi - 110 003, India*

(*Received 22 April 2024, Accepted 17 July 2024*)

e mail :anand.shankar@imd.gov.in

सार– कोहरे के कारण आम तौर पर वातावरण में दृश्यता कम हो जाती है। सीमित दृश्यता का परिवहन, विशेष रूप से विमान संचालन पर महत्वपूर्ण प्रभाव पड़ता है। कम दृश्यता का सटीक पूर्वानुमान मुख्य रूप से हवाई अड्डे की गतिविधियों की कुशल योजना आदि विमानन सेवाओं के लिए आवश्यक है। परिष्कृत संख्यात्मक मौसम पूर्वानुमान (NWP) मॉडल के उपयोग के बावजूद, कोहरे और सीमित दृश्यता का पूर्वानुमान चुनौतीपूर्ण बना हुआ है। कोहरे की पूर्वानुमान की जटिलता सूक्ष्म-स्तरीय कारकों को समझने में सीमाओं के कारण है जो कोहरे की उत्पत्ति, तीव्रता, निरंतरता और क्षय का कारण बनते हैं। यह अध्ययन जलवायु संबंधी कम दृश्यता वाले महीनों (नवंबर से फरवरी) में कोहरे (सतह दृश्यता <1000 मीटर) और घने कोहरे (सतह दृश्यता <200 मीटर) की घटना की जांच करता है ताकि कम दृश्यता की घटनाओं की निरंतरता का विश्लेषण किया जा सके और मैंढक प्रवण इंडो-गांगेय मैदान (IGP) क्षेत्रों की विशिष्ट स्थितियों में उनका पूर्वानुमान लगाया जा सके। एक प्रतिनिधि स्टेशन, जय प्रकाश नारायण अंतर्राष्ट्रीय (JPNI) हवाई अड्डा, पटना, भारत में उपकरण गुणवत्ता डेटासेट की उपलब्धता को देखते हुए विचार किया गया है। विश्लेषण में मशीन लर्निंग (एमएल) एल्गोरिदम की विविधता का उपयोग करके श्रृंखला की दीर्घकालिक और अल्पकालिक दृढ़ता और पूर्वानुमान की जांच की जाती है। विस्तारित अवधि में व्यापक विश्लेषण करने के लिए, बड़े पैमाने पर कोहरे और घने कोहरे की समय श्रृंखला के बीच समानता निर्धारित करने के लिए डेट्रेंडेड उतार-चढ़ाव विश्लेषण (डीएफए) का उपयोग किया जाता है। बाइनरी टाइम सीरीज़ को देखने और यह पता लगाने के लिए मार्कोव चेन मॉडल का उपयोग किया जाता है कि अल्पावधि (1-5 घंटे) में कम दृश्यता वाली घटनाएँ (जैसे कोहरा और घना कोहरा) कितने समय तक चलती हैं। अंततः, हम कम दृश्यता (कोहरा या घना कोहरा) के उदाहरणों के लिए एक से पांच घंटे के अग्रकाल के साथ एक तात्कालिक पूर्वानुमान का विश्लेषण करते हैं। यह तात्कालिक पूर्वानुमान मार्कोव चेन मॉडल, दृढ़ता विश्लेषण और मशीन लर्निंग (एमएल) विधियों सहित विविध पद्धतियों का उपयोग करके उत्पन्न की जाती है। अंत में, स्थापित करें कि इस पूर्वानुमान समस्या में सबसे अनुकूल और विश्वसनीय परिणाम विशेषज्ञों के मिश्रण मॉडल को नियोजित करके प्राप्त किए जाते हैं जो दृढ़ता-आधारित विधियों और एमएल एल्गोरिदम को एकीकृत करता है।

ABSTRACT. Fog typically results in reduced atmospheric visibility. Severely limited visibility has a significant impact on transportation, particularly the operations of aircraft. Precise forecasts of low visibility are essential for aviation services, primarily for the efficient planning of airport activities. Despite the utilization of sophisticated numerical weather prediction (NWP) models, the prediction of fog and limited visibility remains challenging. The intricacy of fog prediction is due to limitations in understanding the micro-scale factors that lead to fog genesis, intensification, persistence, and dissipation. This study investigates the occurrence of fog (surface visibility <1000 m) and dense fog (surface visibility <200 m) throughout the climatological low-visibility months (November to February) to analyze the persistence of low-visibility events and predict them in the specific conditions of the fog prone Indo-Gangetic Plain (IGP) regions. A representative station, Jay Prakash Narayan International (JPNI) Airport in Patna, India, has been considered given the availability of instrumental quality datasets. The analysis investigates the long-term and short-term persistence and prediction of the series using a diverse variety of machine learning (ML) algorithms. To conduct a comprehensive analysis over an extended period, detrended fluctuation analysis (DFA) is employed to determine the similarities between the time series of large-scale fog and dense fog. A Markov chain model is used to look at the binary time series and figure out how long low-visibility events (like fog and dense fog) last in the short term (1-5 hours).

Ultimately, we analyze a short-term forecast (Nowcast) with a lead time of one to five hours for instances of low visibility (fog or dense fog). This nowcasting is generated utilizing diverse methodologies, including Markov chain models, persistence analysis and machine learning (ML) methods. Finally, establish that the most favorable and reliable results in this prediction problem are attained by employing a Mixture of Experts model that integrates persistence-based methods and ML algorithms.

Key words- Aviation services, The potential of persistence, Machine learning algorithms, The nowcasting of low-visibility events.

1. Introduction

Low visibility caused by fog (surface visibility <1000 meters and relative humidity >90%) (IMD, Ministry of Earth Sciences, 2021; World Meteorological Organization, 2019) and dense fog (surface visibility < 200 m) are highly unfavorable weather conditions for the operations of airports, mainly during the landing and take-off of the flight (Fernández-González *et al*., 2019; Haeffelin *et al*., 2016; Shankar and Sahana, 2023b). (Herman and Schumacher, 2016; Pahlavan *et al.*, 2021; Singh *et al.*, 2018; Singh and Kant, 2006; Stolaki *et al.*, 2009) have identified it as one of the most challenging weather conditions because it significantly reduces the capacity of airport operations, especially runways (Guijo-Rubio *et al.*, 2018; Mohan *et al.*, 2015). To mitigate the risk of runway incursions and other potential incidents or accidents that may occur during low-visibility events (fog or dense fog), air traffic controllers may impose limitations on the use of taxiways, increase the time interval between takeoffs and landings, or, in extreme cases, suspend airport operations altogether (Hosea, 2019; Koyuncu *et al.*, 2022*)*. The occurrence of mishaps with low visibility has greatly increased due to the surge in aviation traffic in recent decades (Gultepe *et al.*, 2007; Lakra and Avishek, 2022). Airport Traffic Management (ATM) implements specific low-visibility procedures (LVP) to ensure the safety of operations at the airport under low-visibility occurrences (Shankar and Giri, 2024). Subsequent decreases in visibility may necessitate a temporary cessation of airport operations or the temporary closure of the airport. Furthermore, the rates of missed approaches are increasing, which creates a burden and pressure on ATM officials. Consequently, meteorological officials associated with aviation services frequently encounter difficulty in accurately forecasting low visibility (Kutty *et al*., 2019; Parde *et al*., 2022; Pithani *et al*., 2019). Nevertheless, this is an exceedingly difficult undertaking that requires a thorough knowledge of the topographical features of the area and a comprehension of the meteorological processes that influence the onset or dissipation of low visibility (fog or dense fog) (Da Rocha *et al*., 2015; Müller *et al*., 2010). To assist forecasters in improving their ability to predict occurrences of low visibility specific to aviation services, numerous strategies have been developed. Numerical weather prediction has gained significant popularity as a methodology to predict low-visibility (fog or dense fog) events. Several authors (Román-Cascón *et al*., 2012; Román-Cascón *et al.*, 2019; Singh *et al.*, 2018; Van Der Velde *et al.*, 2010) have pointed out that numerical weather prediction isn't very good at predicting when low visibility events (fog or dense fog) occur because fog is very sensitive to small-scale changes specific to the local conditions, like topography, wind speed, or the stability of the atmosphere. Also, NWP requires very high-end computing facilities whose operations are expensive and time-consuming (Dhangar *et al*., 2021; Niu *et al*., 2010; Smith *et al*., 2018). Alternative methodologies involve employing statistical techniques to forecast occurrences of low visibility (Román-Cascón *et al.*, 2016). Initially, linear regression was used as an approach to predict low-visibility events (Koziara, *et al*., 1983). However, the advancement of machine learning (ML) has led to the development of more effective algorithms for predicting these challenging events. These algorithms utilize non-linear methodologies such as artificial neural networks (Cornejo-Bueno *et al.*, 2021; Fabbian *et al*., 2007; Miao *et al*., 2020), fuzzy logic (Miao *et al.*, 2012), Bayesian networks (Boneh *et al.*, 2015; Chmielecki and Raftery, 2011), or support vector machines (Cornejo-Bueno *et al*., 2017; Lo *et al*., 2020) to achieve higher accuracy and reliability. Although there has been much research on different prediction methods, many causative factors of low-visibility events and the optimization of the models have not been adequately utilized in the development of low-visibility forecasting systems. Low-visibility events (fog or dense fog) are persistent (Price *et al.*, 2015). The persisting nature of these occurrences is widely recognized, although less research has been conducted on harnessing the potential of these predictive systems (Pérez-Ortiz *et al.*, 2018; Salcedo-Sanz *et al.*, 2021a). Recent studies have focused on various aspects of weather, such as rainfall, hydrology, wind, sea surface temperature, and solar radiation. Some specific studies have been conducted on rainfall and hydrology (Pelletier and Turcotte, 1997; Yang and Fu, 2019), on the wind (Gadian *et al.*, 2004; Jiang, 2018; Koçak, 2008), on sea surface temperature (Monetti and Havlin 2003; Zhang and Zhou, 2015) and solar radiation (Voyant and Notton, 2018). However, low visibility events (fog and dense fog) have not been extensively studied and documented in the fog-prone IGP regions of India, except a few studies in mid-latitude countries (Belo-Pereira and Santos, 2016; Cornejo-Bueno *et al*., 2020; Guijo-Rubio *et al.*, 2018; Salcedo-Sanz *et al*., 2021a). None of these types of studies have been carried out in the specific context of the fog - prone Indo - Gangetic Plains (IGP).

The studies have found that low visibility events have been occurring frequently, particularly in the Indo-Gangetic Plain (IGP) of the Indian subcontinent, which has different onset and dissipation mechanisms for low-visibility events than mid-latitude countries (Parde *et al*., 2022; Smith *et al*., 2023). Below is a succinct overview of the study's primary objectives and contributions while underscoring the novelty and distinctiveness of the research outcomes.

- Investigating the persistence of low-visibility events in the fog-prone Indo-Gangetic Plains (IGP) regions, both in the long-term and short-term, to develop a comprehensive understanding of their dynamics.

- Introducing a novel approach termed Mixture of Experts (MoE) time series models that seamlessly integrate the persistence characteristics of low-visibility events with advanced machine learning (ML) techniques. This innovative model not only enhances robustness but also offers efficient computational performance, requiring minimal resources for implementation.

- Proposing an alternative forecasting technique for low-visibility events with a lead time of up to 5 hours, showcasing superior accuracy compared to existing methods such as persistence models and traditional ML approaches. This research underscores the effectiveness of the MoE model in achieving higher accuracy and reliability in low-visibility event forecasting.

- The subsequent sections of the paper are structured in the following manner: Following Section 2 gives a brief overview of the dataset. Section 3 with an explanation of the methodologies taken into consideration for this analysis, Section 4 provides results about the persistence of low-visibility events over long and short periods. Section 5 presents the primary discoveries of this investigation and finishes the report with some concluding reflections on this research. Please note that a list of acronyms has been appended to the article for enhanced readability.

2. Study areas and dataset

2.1. *Study areas*

The specific sites within the Indo-Gangetic Plain (IGP) regions, which are sandwiched between the southern Plateau and the Northern Himalaya (as shown in Fig. 1) (Shankar *et al*., 2022), are the focus of analysis of the persistence of the low-visibility events (fog or dense fog) and proposed nowcasting using a mixture of expert models by combining the ML and analysis of persistence models of the low-visibility events (fog and dense fog). The sites of Jay Prakash Narayan International (JPNI) Airport, which lies in the IGP region, have been taken into consideration for the evaluation of the proposed models. There are two primary justifications for this particular choice: The Automatic Weather Observing Station (AWoS) facilitates ongoing surveillance of meteorological data sets, encompassing visibility measurements that offer ample training data for our models (Shankar and Sahana, 2023b). Furthermore, limited visibility leads to notable social and economic repercussions in the IGP regions (Kulkarni *et al*., 2019; Sawaisarje *et al*., 2014). Low-visibility incidents have had a significant negative impact on the operational effectiveness of aviation services in recent years, causing delays, rescheduling, diversion, and cancellations of flights (Shankar and Sahana, 2023a). Hence, the provision of precise forecasts about the prediction of low-visibility events in advance of one to five hours can effectively contribute to the mitigation and improvement of the economic repercussions experienced by aviation services.

2.2. *Dataset*

The instrumental quality hourly surface visibility and associated meteorological parameters of the JPNI Airport Patna (the representative station of the IGP regions) for the climatologically low visibility month (November to February) for the entire period November 2014 to February 2023 (36 months). In these four months (November to February) of a calendar year, radiation, advection and combinations of these two are at their most severe stages. An analysis was conducted on the datasets to determine the long-term and short-term persistence of fog (surface visibility < 1000 m) and dense fog (surface visibility < 200 m) in the time series. As per World Meteorological Organization (WMO) guidelines, the accuracy of the instruments is checked regularly for the target. Variables *i.e*. low visibility events (fog and dense fog) which are measured by the visibility instruments (Transmissometers or scatter meter), as well as the surface meteorological parameter taken from the Automatic Weather Observing System (AWoS) at Patna Airport. The IMD's certification standards are 0.1 °C for air temperature and 1% for relative humidity, 0.2 m/s for wind speed, and 0.5 mm for precipitation *etc*. Input features outlined in Table 1, along with time, are utilized as inputs in the ML algorithms to predict the occurrence of low visibility (fog or dense fog). These variables are selected based on their relevance, feature selection methods based on principal component analysis (PCA), and local knowledge of the mechanisms of the onset and dissipation of low-visibility events (fog or dense fog). The correlation heat map for the optimal feature settings is depicted in Figs. 2 (a) and (b) for fog and dense fog, respectively. The data clearly shows a positive

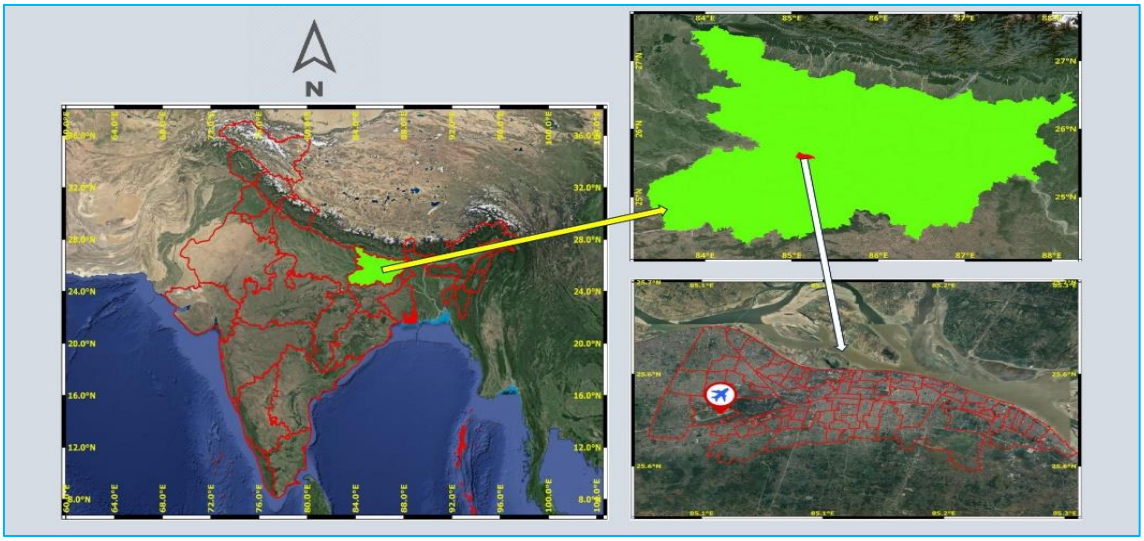

Fig. 1. This illustrates the geographical position of the JPNI Airport Patna, India.

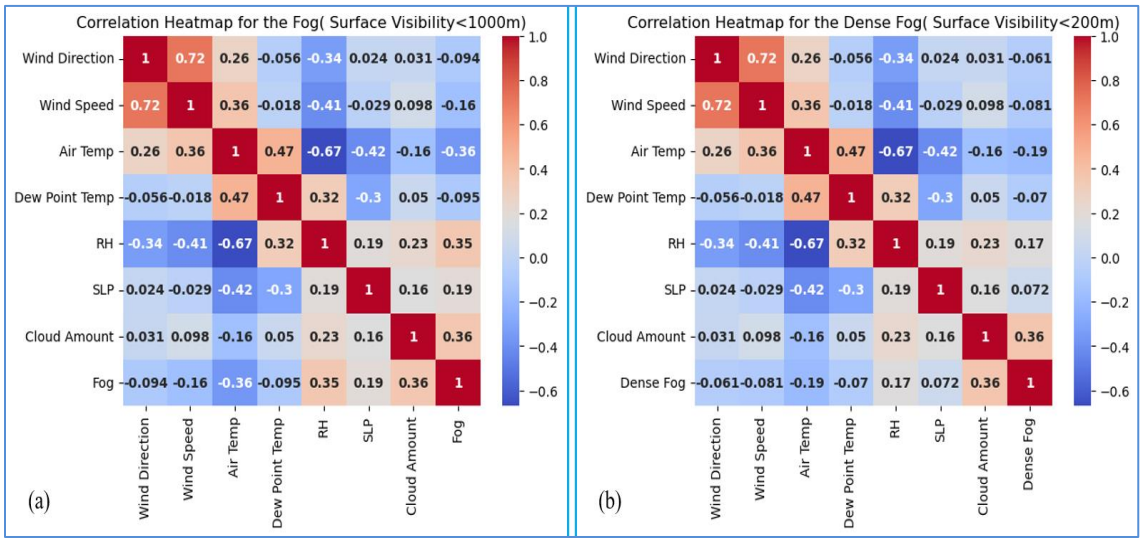

Figs. 2 (a & b). Correlation heat map with the selected meteorological feature with (a) fog and (b) dense fog.

TABLE 1

Details of the target low visibility (fog or dense fog) and the associated meteorological features utilized in the proposed study

Type	Input Features /Target Variables	Unit	Value Range
Meteorological Data as Input	Dry Bulb Temperature	°C	0-34
	Dew Point Temperature	°C	0-24.9
	Relative Humidity	%	13.6 -100
	Wind Speed	knots	0-25
	Wind Direction	Degrees	0-360
	Station Level Pressure	hPa	998.2-1019.1
	Visibility	m	0-8000
Target (Low Visibility)	Fog	Surface visibility<1000 m	40 hours (Highest persistence)
	Dense Fog	Surface Visibility<200 m	13 hours (highest Persistence)

Source : India Meteorological Department

correlation between fog and dense fog and meteorological parameters such as relative humidity, station level pressure and cloud amount. Conversely, there is a negative correlation with wind direction, wind speed, air temperature and dew point temperature. The cloud amount, air temperature and relative humidity have the highest correlation coefficients. To enhance the Naive persistence prediction, we used five previous time steps (time windows for input variables) to consider these predictive parameters (t-1, t-2, t-3, t-4 and t-5).

3. Methodology

The primary contribution of this work is to present a prediction based on the best suitable combination using the potential of persistence and machine learning for low-visibility (fog and dense fog) events with a lead time of 1 to 5 hours. Also, the suggested mixture of expert (MOE) models enhances the performance of the machine learning models by incorporating the potential of persistence in situations of low visibility. The suggested methodology has a high potential for practical application in the forecasting of critical low-visibility (fog or dense fog) events in aviation services. Fig. 3 depicts the methodology used for analyzing persistence and predicting low visibility in real time. All the ML models and their proposed Mixture of Experts (MOE) models have been developed using the Python programming language on the Anaconda Platform. The details methodology used in the analysis of the persisting nature of low-visibility long-term and short-term persistence is outlined in the subsequent subsection. The evaluation of the performance of these models is conducted by utilizing the performance metrics outlined in sub-section 3.4.

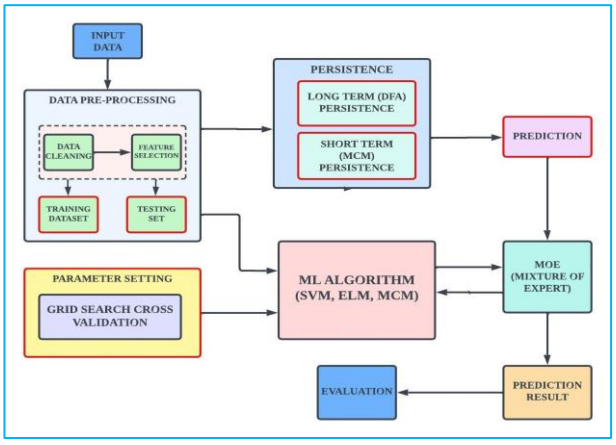

Fig. 3. Illustrates the process block diagram for analyzing and predicting low visibility (fog or dense fog) using persistence. The detailed procedures (step by step) of the applied methodology (data input, data preprocessing, persistence, parameter setting (model optimization), prediction, proposed MOE, and model evaluation) in the predictions of the low-visibility events (fog and dense fog).

3.1. *Long-term persistence: detrended fluctuation analysis*

The detrended fluctuation analysis (DFA) approach is a robust tool for identifying the scaling properties of long-term persistence based on the inherent dynamics of time series. This highly effective technique may accurately identify and eliminate any misinterpretations included in the data sets. (Peng, *et al*., 1994) pioneered the use of the DFA approach for analyzing DNA time series. (Bunde, *et al*., 2000) and (Kantelhardt, *et al*., 2001) expanded and broadened the DFA approach. The DFA approach has been utilized in various fields, such as temperature records (Talkner, 2000; Blender, 2003; Govindan, *et al*., 2002), precipitation processes (Jiang and Li, 2017), relative humidity records (Chen and Lin, 2007) and SST (Luo, *et al*., 2015), among others. The DFA algorithm consists of three primary phases (Hu *et al*., 2001). Begin by eliminating the recurring patterns in time series data for fog and no fog, as well as dense fog and no dense fog, represented as binary values (0 or 1).

The time series profile Y_j is subsequently established in the following manner:

$$Y_j = \sum_{i=1}^{j} x_i \tag{1}$$

The profile Y_j is divided into Ns $=\left|\frac{N}{s}\right|$, non-overlapping segments $\{Y_j^k | 1 \le k \le Ns\}$ of equal length s.

Also, determine the local least squares straight line, which assesses the local trend of each element. As a result, the piece-wise functions are obtained by compounding each linear fitting.

$$\tilde{Z}_j^s = [Z_j^1 \ldots . Z_j^k \ldots . Z_j^{N_s}] \tag{2}$$

The superscript "s" represents the period for the linear fitting of each segment.

- Then, by varying the temporal window length s, the fluctuation is obtained as the root-mean-square error obtained from this linear piece-wise function and the profile Yj:

$$F(s) = \sqrt{\frac{1}{N}\sum_{k=1}^{N}(\tilde{Z}_j^s - Y_j)^2} \tag{3}$$

The function F(s) increases as the time windows follow the power law $F(s) \propto s^{\alpha}$ within a stable range of time scales. The scaling exponent α, sometimes referred to

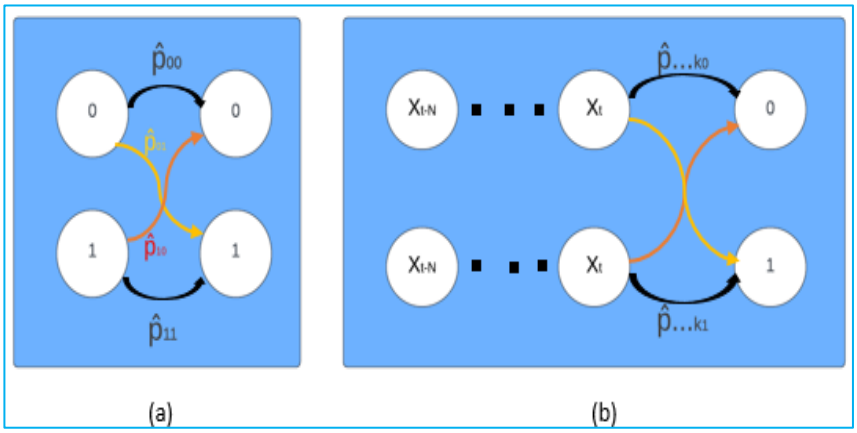

Figs. 4 (a & b). Represents a binary system (a) First-order (b) N-order Markov process.

as the correlation exponent, represents the gradient of the linear regression line that has been fitted. The Hurst exponent (H) and the scaling exponent α in the DFA technique are equivalent concepts that have the same interpretation in this particular situation (Graves *et al.*, 2017). The Hurst coefficient, denoted as H (or α in this case), provides a quantification of the potential simple power-law scaling of the power spectrum S(f) with frequency f. It is commonly used as an indicator of the long-term persistence of time series, which is frequently described as "self-similar" behavior (Mann, 2011).

$$S(f) \sim f^{-\beta} \tag{4}$$

Where, the scaling exponent β is β = 2α-1.

It is important to highlight that the time series is uncorrelated when the coefficient α = 0.5, demonstrating the absence of long-term persistence in the time series. For values (0.5 < α ≤ 1), the time series exhibits positive long-term correlation. This indicates that there is long-term persistence within the proper range of scales. The process exhibits anti-persistence when the value 0 < α ≤ 0.5. When α > 1, the persistence is high enough to cause the time series to exhibit non-stationary behavior.

3.2. *Short-term persistence: markov chain models (mcms)*

Various statistical techniques have been used for weather forecasting (Wilks, 2011). MCMs are statistical techniques employed for the short-term forecasting of meteorological data series. Due to their utilization of localized meteorological data, MCMs possess a reduced computing burden and the capability to promptly provide forecasts after measurements (Cazacioc, 2005). In the subject of meteorology, various interconnected processes can be understood by considering fundamental first-order Markov chain models *(e.g.* temperature, precipitation, *etc*.) (Chatfield, 1973; Fowler, 2007). In the current situation of low-visibility events, consider a discrete binary variable that has two alternative states. When the time series for fog or dense fog is converted into a binary variable, it can indicate either the occurrence of fog (value 1) or the absence of fog (value 0). The probability of fog occurring on an hourly basis can be categorized into four conditions based on the assumption that the current likelihood of fog is dependent on the fog occurrence in the preceding hour. This assumption follows the principles of a first-order Markov chain (Katz, 1977). Fig. 4 illustrates a schematic diagram explaining the characteristics of a first-order and N-order MCM.

$$\begin{aligned} p_{00} &= P(X_{t=0}|X_{t-1=0}) \\ p_{01} &= P(X_{t=1}|X_{t-1=0}) \\ p_{10} &= P(X_{t=0}|X_{t-1=1}) \\ p_{11} &= P(X_{t=1}|X_{t-1=1}) \end{aligned} \tag{5}$$

By utilizing the conditional relative frequencies, the transition probabilities are calculated as follows:

$$\hat{p}_{00} = \frac{n_{00}}{n_0} \hat{p}_{01} = \frac{n_{01}}{n_0} \hat{p}_{10} = \frac{n_{10}}{n_1} \hat{p}_{11} = \frac{n_{11}}{n_1} \tag{6}$$

In equation (6), n_{ij} represents the count of transitions from state i to state j and n_i represents the count of occurrences of state i followed by any other data point. Specifically, $n_i = n_{i0} + n_{i1}$. The subscripts, i, j ∈{ 0, 1}, correspond to the state. The Naive persistence operator can be classified as a first-order Markov chain model, where the formula x (t + 1) = x(t) ensures that the state is preserved at any given time. The following transition probability matrix is an alternative way to represent it:

$$P = \begin{bmatrix} 1 & 0 \\ 0 & 1 \end{bmatrix} \tag{7}$$

The transition probabilities of a higher-order Markov chain model take into account the time frames under

consideration. Higher-order chains violate the memoryless property of first-order Markov chains. Second-order Markov chains incorporate the states at periods t-2 and t-1 to forecast the state at time t. Similarly, the third-order Markov chain considers the states at times t-3, t-2 and t-1 to predict the state at time t. The transition probabilities are stated as follows:

$$p_{i_2 i_1 \to i} = P(X_t = i | X_{t-1} = i_1, X_{t-2} = i_2) \quad i, i_1, i_2 \in \{0, 1\} \tag{8}$$

$$p_{i_3 i_2 i_1 \to i} = P(X_t = i | X_{t-1} = i_1, X_{t-2} = i_2, X_{t-3} = i_3), \quad i, i_1, i_2, i_3 \in \{0, 1\} \tag{9}$$

For higher orders:

$$p_{\alpha \to i} = P(X_t = i | X_{t-1} = \alpha_1, \ldots X_{t-N} = \alpha_N), \quad i \in \{0, 1\}, \alpha = (\alpha_1, \ldots \alpha_N) \in \{0, 1\}^N \tag{10}$$

α is a tuple consisting of N elements that encompass all considered time frames.

3.3. *Machine learning algorithms for classification tasks*

This study employs advanced ML algorithms as classification tasks, specifically Support Vector Machines (SVMs) and Extreme Learning Machines (ELMs), to predict the occurrence of fog/no fog or dense fog/no dense fog in the specific condition of the IGP regions, *i.e.*, Patna Airport, India. These algorithms have been proven to be effective in similar research (Cristianini and J., 2000; Salcedo-Sanz *et al.*, 2014; Sumathi and Paneerselvam, 2020). Support Vector Machine (SVM) is a widely recognized statistical learning technique built on kernels (Schölkopf and Smola, 2002). The ELM is a very efficient and quick-to-train algorithm that relies on a pseudo-inverse calculation. It is important to note that the algorithms used in this study are specifically designed to address classification tasks (Ding *et al.*, 2014; María *et al.*, 2016).

3.3.1. *Support vector machine*

The standard Support Vector Machine (SVM) formulation is known as a maximum margin classifier. This means that the SVM's decision function is a hyperplane that effectively separates samples from different classes. In this context, class 1 represents a state of either fog (surface visibility <1000 m) or dense fog (surface visibility < 200 m), while class -1 (equivalent to 0) represents a state of no fog or no dense fog. The SVM approach addresses the following challenges: given a labeled training dataset. $\{(x_i, y_i)\}^n{}_{i=1}$, where xi ∈ R^N and y_i ∈{-1, +1}, and given a non-linear mapping $\Phi(.):R^N \to R_p (N<<p)$. $\Phi(.):R_N \to R_p$ (N<<p).

$$\underbrace{min}_{w,b,\zeta} \frac{1}{2}||w|| + C \sum_{i=1}^{N} \zeta i \tag{11}$$

s.t. $y_{i((w,\Phi(xi))+b)+\zeta i}-1 \geq 0; \quad i = 1, \ldots, n$

$\zeta i \geq 0$ I = 1,2,..,n

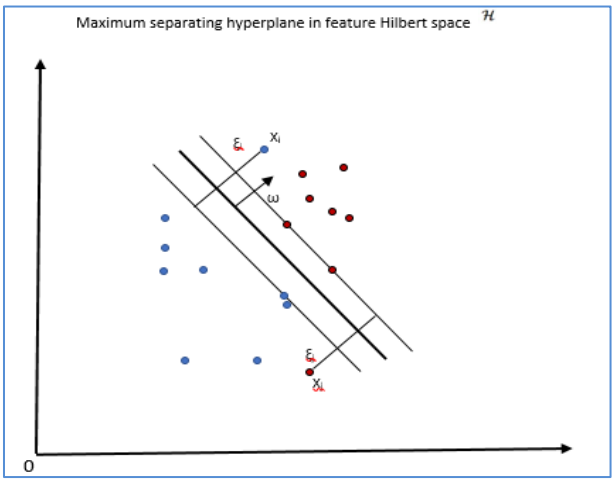

Fig. 5. Linear decision hyperplane in a non-linearly modified feature space H. The soft margin is defined by including the slack variables ζ_i.

The positive slack variables ζ_i are used to account for acceptable mistakes. The parameters w and b, shown in Fig. 5, represent the separating hyperplane R^N.

where, ζi are positive slack variables allowing for the handling of permissible errors and w and b constitute a separating hyperplane in R^N, shown in Fig. 5.

The objective function of Equation (11) comprises two terms with distinct interpretations. One term aims to minimize the accumulated errors, $\sum_{i=1}^{n} \zeta_i$, while the other term minimizes the Euclidean norm of the model weights, ||w||2. This norm can be shown to be equivalent to maximizing the margin, which represents the separation between classes. It is important to note that the hard margin of the SVM can be achieved by solely maximizing the margin without considering errors in the objective function. Adding the slack variables ζi, dealing with data that can't be separated, and using the soft margin SVM method can help solve the problem. This method lowers the training error traded off against the margin. It's more likely that the transformed samples can be separated linearly in the higher-dimensional feature space R^p (N<<p) if the right non-linear mapping $\Phi:R^N \to R^p$ is chosen appropriately. The user is usually required to modify the regularization hyper parameter C, which controls the classifier's ability to generalize. According to (Schölkopf and Smola, 2002), Equation (11)'s dual problem counterpart resolves the main issue. This leads to the decision function displayed below for any test sample $x* \in R^N$:

$$f(x*) = sgn\left(\sum_{i=1}^{n} y_i \, \alpha_i K(xi, x*) + b\right) \tag{12}$$

The Lagrange multipliers α_i correspond to the restrictions of the primary issue (12). The training samples xi with non-zero Lagrange multiplier αi ≠ o are referred to as support vectors (SVs). The function K (x_i, $x_{*)}$ represents the scalar product of the high-order space R_p, which is mapped to the sample space. The test sample, x*, is projected onto the support vector, x_i, which is then transformed into a higher-dimensional space. The bias term b is subsequently calculated by applying any of the constraints that are relevant to an unbounded Lagrange multiplier.

$$b = \frac{1}{k}\left(\sum_{i=1}^{k} y_i - (\Phi(x_i), w)\right) \quad (13)$$

where, k is the total number of unbounded Lagrange multipliers (*i.e.*, $0<\alpha_i<C$) and

W = $\sum_{i=1}^{n} y_i \alpha_i \Phi(x_i)$ (Schölkopf and Smola, 2002)

3.3.2. *Extreme Learning Machines*

The training of feed-forward perceptron structures can be expedited by utilizing neural networks with an extreme-learning machine, as presented in Fig. 6 (Huang *et al.*, 2015). The hidden-layer output matrix is transformed into a pseudo-inverse by randomly assigning network weights to the first layer of the ELM. The optimal weights for the output layer are derived by utilizing the pseudo-inverse, which effectively fits the objective values. The advantage of this strategy is in its efficiency and ability to yield outcomes that are on par with other established methodologies, such as conventional multi-layer perceptron training and SVM algorithms. The ELM's ability to universally approximate has been proven (Ding *et al*., 2014; Huang *et al*., 2006).

The ELM technique can be defined as follows, considering a training set. { (x_i, y_i) | $x_i \in R^N$, $y_i \in \{-1,+1\}$,$1 \le i \le n$}, an activation function g(x), and a present number of hidden nodes $\widehat{N}$.

(i) Randomly assign the ELM weight value (w_i) and the bias (bi) using a uniform probability distribution in the range [-1, 1], where i = 1,..., N.

(ii) Calculate the hidden-layer output matrix H using the following formula:

$$H = \begin{bmatrix} g(w_1 x_1 + b1) & \cdots & g(w_{\widehat{N}} x_1 + b_{\widehat{N}} \\ \vdots & \ddots & \vdots \\ g(w_1 x_n + b1) & \cdots & g(w_{\widehat{N}} x_n + b_{\widehat{N}} \end{bmatrix} \quad (14)$$

(iii) Next, calculate the output weight vector β by applying the formula:

$$B = H^{\dagger}T \quad (15)$$

The matrix H is the Moore-Penrose inverse of H and the training output vector T is represented as, $T=[y_1,\ldots y_n]^T$.

It is important to mention that the ELM algorithm requires the specification of the free parameter $\widehat{N}$ before training. To achieve good results, an approximation of $\widehat{N}$ must be obtained by scanning a range of $\widehat{N}$.

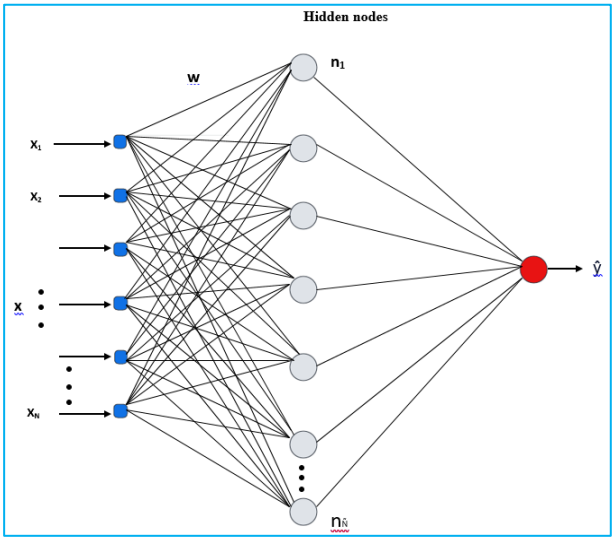

Fig. 6. The details of the Extreme Learning Machine (ELM) algorithm architecture which incorporates a multi-layer perceptron structure.

3.4. *Performance metrics*

The statistical metrics of accuracy (ACC), true positive rate (TPR), true negative rate (TNR) and F1 score were used to assess the proposed methods and their benchmarked prediction models. For this study, occurrences of fog and dense fog are each represented by a positive condition (state 1) that equates to surface visibility of <1000 m or <200 m respectively. On the other hand, the absence of fog or dense fog is represented by the binary variable connected to surface visibility ≥1000 m or ≥ 200 m (state 0 or -1) for ML algorithms. The notation used in the calculations describes the statistical measures. P number of real positives; N number of real negatives; TP is true positive; TN is true negative; FP is false positive; FN is false negative.

ACC shows how close to the actual time series are the predicted time series. It is calculated as:

$$ACC = \frac{TP+TN}{P+N} \quad (16)$$

TPR is a measurement that determines the percentage of actual positives that are accurately identified as positives(Fawcett, 2006):

$$TPR = \frac{TP}{TP+FN} \quad (17)$$

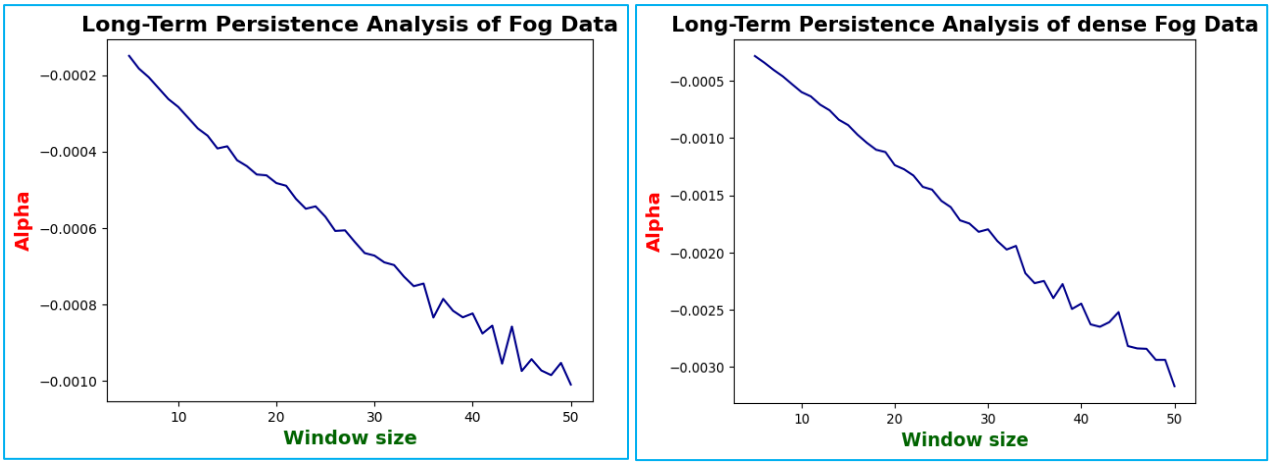

Fig. 7. Detrended Fluctuation Analysis (Plot between alpha and window size) carried out for the entire time series data of (a) fog and (b) dense Fog for the representative site of IGP regions, *i.e.*, Patna Airport. The plots depict that the fog has a noticeable long-term anti-persistent nature.

TNR is a measurement that determines the percentage of actual negatives that are accurately identified as negatives:

$$TNR = \frac{TN}{TN+FP} \tag{18}$$

The F1 Score is a measurement of the accuracy of a test, and it reaches its optimal value at 1 (Sasaki, 2007).

$$F1S = \frac{2TP}{2TP+FP+FN} \tag{19}$$

4. Results

In this section, the results of the analysis of the long and short-term persistence of low-visibility events (fog or dense fog) have been presented along with the proposed mixture of experts (MOE), which is a combination of the ML-based and persistence-based models for the nowcasting of low-visibility events (fog or dense fog) in the specific condition of the IGP regions (representative stations: Patna, India). Long-term and short-term persistence are differentiated based on the diverse sorts of analyses involved. To ensure long-term persistence, we present the findings of the DFA technique, which provides the correlation exponent (α) (discussed in sub-section 3.1). The MCM transition probabilities (discussed in Subsection 3.2) are utilized to examine the short-term persistence. In addition, to address the problem of predicting short-term low-visibility events (fog or dense fog), *i.e.*, now casting, the proposed MOE models incorporate the best prediction information from ML-based and persistence-based models. Also, compare the accuracy of MCM and benchmarked ML models with the Naive persistence operator (x (t + 1) = x(t)). The Naive persistence operator is a powerful solution at the hourly scale. The implementation code was written in Python 3.10. The proposed MOE models are developed on a laptop with a Windows 11 operating system and an Intel (R) Core (TM) i5-1035G1 processor running at 1.00 GHz and 8 GB of memory.

4.1. *Long-Term Persistence Analysis*

The DFA algorithm, as outlined in subsection 3.1, is utilized to analyze the complete time series spanning from 2014 to 2023. Specifically, this analysis focuses on the climatologically foggy seasons (November, December, January and February) of the IGP Regions. The datasets under examination pertain to both fog (surface visibility < 1000 m) and dense fog (surface visibility < 200 m). The objective of this analysis is to evaluate the long-term persistence of fog and dense fog conditions. Fig. 7 illustrates the relationship between alpha and window size for both (a) fog and (b) dense fog of the IGO regions (representative sites: Patna Airport). The plot amply demonstrates that both fog and dense fog exhibit anti-persistence, as the auto-correlation is close to 0.

4.2. *Short -Term Persistence Analysis*

In this study, two types of fog events are looked at: fog/no fog (1, 0) and dense fog/no dense fog (1, 0). These are looked at in terms of both short-term persistence analysis and following low-visibility event prediction as classification problems. Consequently, it is necessary to convert the fog and dense fog events into binary form. The results of the analysis discuss the findings of the problem related to predicting fog and dense fog in the specific conditions of the IGP regions. To maintain the integrity of the results despite the division of data into training and test sets, a K-fold cross-validation technique was employed (Kohavi, 1995). A value of K = 5 has been selected for the folding process, indicating that 80% of the

TABLE 2

Probabilities of transitions in the first-order Markov Chain Models (MCM) for fog and dense fog events

$P = \frac{1}{2}(p_{00} + p_{11})$	0(No Fog)	1(Fog)	0(No Dense Fog)	1(Dense Fog)
0	**0.9774**	0.0225	**0.9945**	0.0054
1	0.1767	**0.8232**	0.2506	**0.7494**

TABLE 3

Probabilities of transitions in the 2nd-order Markov Chain Models (MCM) for fog and dense fog events

$P = \frac{1}{2}(p_{00\to0} + p_{11\to1})$	0 (No Fog)	1 (Fog)	0 (No Dense fog)	1 (Dense Fog)
00	**0.9777**	0.0222	**0.9949**	0.0050
01	0.1861	0.8138	0.2222	0.7777
10	0.9652	0.0347	0.9259	0.0740
11	0.1747	**0.8252**	0.2600	**0.7399**

TABLE 4

Probabilities of transitions in the 3rd order Markov Chain Models (MCM) for fog and dense fog events

$P = \frac{1}{2}(p_{000\to0} + p_{111\to1})$	0 (No Fog)	1 (Fog)	0 (No Dense fog)	1 (Dense Fog)
000	**0.9775**	0.0224	**0.9948**	0.0051
001	0.1825	0.8174	0.21	0.79
010	0.92	0.08	0.875	0.125
011	0.1676	0.8323	0.2261	0.7738
100	0.9871	0.0128	1	0
101	0.2857	0.7142	0.375	0.625
110	0.9756	0.0243	0.9404	0.0595
111	0.1762	**0.8237**	0.2719	**0.7280**

data will be allocated for training and the remaining 20% will be used for testing. In addition, the short-term prediction results presented in the following section were derived from the same data partition used for this persistence analysis. The matrix of transition probabilities obtained from the Markov Chain Model (MCM) discussed in subsection 3.2 will be utilized to assess the short-term persistence. The persistence can be approximated by using the components of the major diagonal as follows:

$$p = \frac{1}{2}(p_{00} + p_{11}) \tag{20}$$

Estimate the short-term persistence of higher-order MCM as follows:

$$p = \frac{1}{2}(p_{\alpha^0\to0} + p_{\alpha^1\to0}) \tag{21}$$

where, α^0 = (0,…. 0) indicates an N-element tuple with value 0, and α^1 = (1,…. 1) denotes an N-element tuple with value 1.

TABLE 5

Probabilities of transitions in the 4th order Markov Chain Models (MCM) for fog and dense fog events

$P = \frac{1}{2}(p_{0000\to0} + p_{1111\to1})$	0 (No Fog)	1 (Fog)	0(No Dense fog)	1 (Dense Fog)
0000	**0.9774**	0.0226	**0.9950**	0.0050
0001	0.1849	0.8151	0.2100	0.7900
0010	0.9296	0.0704	0.8571	0.1429
0011	0.1635	0.8365	0.1899	0.8101
0100	0.9710	0.0290	1.0000	0.0000
0101	0.3333	0.6667	0.6667	0.3333
0110	0.9818	0.0182	0.8947	0.1053
0111	0.2308	0.7692	0.2462	0.7538
1000	0.9844	0.0156	0.9800	0.0200
1001	0.0000	1.0000	nan	nan
1010	0.7500	0.2500	1.0000	0.0000
1011	0.3000	0.7000	0.8000	0.2000
1100	0.9906	0.0094	1.0000	0.0000
1101	0.2500	0.7500	0.2000	0.8000
1110	0.9744	0.0256	0.9538	0.0462
1111	0.1646	**0.8354**	0.2816	**0.7184**

The transition probability and short-term persistence estimation for low visibility events (fog and dense fog) at the representative sites of IGP regions, *i.e*., Patna Airport, are presented as 1st Order MCM (Table 2), 2nd Order MCM (Table 3), 3rd Order MCM (Table 4) and 4th Order MCM (Table 5) on the training dataset.

Low-visibility (fog and dense fog) events have a clear pattern of short-term persistence, which is slightly enhanced when higher-order MCM models are taken into account. Considering the prolonged period of low visibility in the past few hours (specifically, incident 1111→ 1), Table 5 (4th order MCM) indicates that the fog event has lasted for more than 83.54% of the time. The value of the overall persistence P is approximately 91%. However, the persistence of dense fog (1111 → 1) only exhibits a rate of 71.84%, but the overall persistence of dense fog is around 86%. Therefore, it is clear that the duration of fog is increased to a greater extent and a higher degree compared to dense fog. However, in this situation, the likelihood of the low-visibility events persisting (meaning the chance of transitioning from one state to another) is lower for higher-order MCM. Specifically, it is only 82.32% and 74.94%, respectively, as shown in Table 2.

4.3. *Short-term prediction*

In this subsection, the potential of persistence has been tapped along with the ML models by using the Mixture of Experts (MOE) models for the improved performance of the prediction of low-visibility events (as a classification task) at the representative sites of the fog-prone Indo-Gangetic Plains (IGP), *i.e*., Patna Airport. In particular, it is worth mentioning that the MCM's probability metric makes it possible to make predictions based only on past events (or the system's binary states). By using a first-order MCM and the transition metrics (Equation 7), the uncomplicated persistence operator performs as a reference prediction technique. As anticipated, it demonstrates excellent performance in predicting fog and dense fog events within an hourly time frame, achieving an accuracy value of 0.9349 and 0.9743, respectively. It is worth mentioning that even when external influences are taken into account, the Naive Persistence Operator still exhibits highly accurate prediction performance at this level of precision. The prediction of low-visibility events by using state-of-the-art ML algorithms by considering the atmospheric conditions and dynamics, proper feature selection and correlation are essential for accelerating prediction and avoiding over fitting by minimizing the number of attributes. To examine the correlation between the low-visibility events (fog and dense fog) and the predictors, the best optimal correlation is presented in Figs. 2 (a & b), respectively. Also, the results of the meteorological parameter after the feature selection are presented in Table 1.

Additionally, the proposed models' performance evaluation metrics are discussed in subsection 3.4. Finally, the Mixture of Experts (MOE) methodology was applied to consider both the persistence and dynamics of atmospheric conditions. The objective of this experiment is to show that, despite the moderate persistence of low-visibility events, hybrid models that integrate both atmospheric conditions and persistence yield the most accurate results for predicting instances of low-visibility events. To compare the results of the baseline approach, which uses the naive persistence operator, with alternative ML algorithms. The input data is analyzed for different periods (t-1, t-2, t-3, t-4 and t-5) or predicted for a lead time of 1 to 5 hours. Both the ELM and SVM techniques may effectively overcome the limitations of the Naive persistence operator, with few differences between them. Improving the effectiveness of machine learning methods is possible by building on the Naive operator and adding other algorithms like ELM, SVM and MCM, along with the proposed MOE system (Pérez-Ortiz *et al.*, 2018), which is a majority voting system. The MOE system, which considers a temporal window of t-1, outperforms all other algorithms in predicting short-term low- visibility events in this challenge. The ELM method, when combined with external atmospheric variables and the MOE, demonstrated the highest level of accuracy among all examined algorithms. Specifically, it achieved accuracy rates of 0.95 and 0.98 for fog and dense fog, respectively, during the time frames of t-2 to t-4. However, throughout the t-5-time window, the accuracy significantly drops for fog detection, particularly in dense fog events. The statistical skill scores of different approaches (MCM, ELM, SVM, naive persistence and proposed MOE) for the prediction of fog (surface visibility <1000 m) and dense fog (surface visibility <1000 m) are presented in Tables 6 and 7, respectively.

TABLE 6

Statistical skill scores of different approaches (MCM, ELM, SVM, Naive persistence, and proposed MOE) for the prediction of fog (surface visibility<1000 m).

Time Window	Model	ACC	TPR	TNR	F1 Score
t-1	MCM	0.9349	0.8357	0.9485	0.9624
	ELM	0.9500	0.8197	0.9699	0.9699
	SVM	0.9537	0.8213	0.9719	0.9737
	MOE	0.9551	0.8199	0.9739	0.9744
t-2	MCM	0.9414	0.8500	0.9540	0.9663
	ELM	0.9537	0.8213	0.9719	0.9737
	SVM	0.9428	0.6420	0.9848	0.9680
	MOE	0.9535	0.8214	0.9721	0.9730
t-3	MCM	0.9487	0.8532	0.9618	0.9706
	ELM	0.9537	0.8213	0.9719	0.9737
	SVM	0.9287	0.4888	0.9890	0.9607
	MOE	0.9541	0.8217	0.9717	0.9733
t-4	MCM	0.9539	0.8516	0.9680	0.9737
	ELM	0.9537	0.8213	0.9719	0.9737
	SVM	0.9212	0.4435	0.9903	0.9565
	MOE	0.9531	0.8313	0.9700	0.9737
t-5	MCM	0.8476	0.6874	0.8696	0.9094
	ELM	0.9212	0.4435	0.9903	0.9565
	SVM	0.9196	0.3907	0.9923	0.9615
	MOE	0.9333	0.5034	0.9701	0.9191
t-1	Naive	0.9551	0.9775	0.8420	0.9744

5. Discussion

The long-term persistence of low-visibility (fog or dense fog) events in the specific conditions of the IGP regions (representative station Patna airport, India) was analyzed using a DFA technique.

The plots between the alpha values for fog (Fig. 7(a)) and dense fog (Fig. 7 (b)) at various window sizes depict

that the dense fog in the IGP regions is anti-persistent. Moreover, as the window size increases, the alpha value decreases in an essentially linear fashion. This indicates that a larger window size is unfavorable for the long-term persistence of low-visibility events. It demonstrates a significant decrease in the persistence of fog beyond 10 hours. There is a strong linkage between the two ranges of the DFA (the window size and pattern of a binary time series (events of fog and no-fog)) that has been studied before (Belo-Pereira and Santos, 2016; S. Cornejo-Bueno *et al*., 2020; Salcedo-Sanz *et al*., 2021b) for the mid-latitude countries. However, in the specific conditions of the IGP regions, the low-visibility events have weak linkages, so they are anti-persistent. Based on this analysis, low-visibility events (fog or dense fog) return periods of 12-13 hours or 22-24 hours in the specific conditions of the IGP regions during the study period (November to February).

Conversely, the analysis of short-term persistence has primarily focused on analyzing the Markov Chain Model (MCM) transition probability metrics at different time intervals. Fog (surface visibility <1000 m) displays significant short-term persistence, with values ranging from 90.03% when considering a one-hour time lag to 90.64% for higher-order MCM with up to four hours of time lag. However, in the short-term persistence of dense fog (surface visibility <200 m), the values ranged from 87.2% for a one-hour lag to 85.67% for a five-hour lag (fourth-order MCM).

Finally, examine several different approaches to ML algorithms (ELM, SVM) and tap the potential of persistence-based models (MCM) to nowcast the low-visibility events (fog and dense fog) for the specific conditions in the IGP regions. After hyper tuning the parameters of the ML algorithms (SVM, ELM) in the specific conditions of the IGP regions with external factors and combining the persistence-based MCM models, the proposed Mixture of Experts (MOE) has superior performance compared to benchmarked models presented in Table 6 (for fog) and Table 7 (for dense fog). Also, the proposed MCM models consistently perform better than the naïve operator model (Presented in Tables 6 and 7). The naïve operator models are based on probability metrics derived from actual low-visibility events.

This indicates a lack of long-term persistence, but for shorter periods, it is highly established. When taking into account ML algorithms (ELM) that incorporate atmospheric variables, the increase in accuracy compared to the basic operator is negligible (0.95 vs. 0.9551) and (0.98 versus 0.97) for fog and dense fog, respectively. This indicates there are no enhancements

TABLE 7

Statistical skill scores of different approaches (MCM, ELM, SVM, Naive persistence and proposed MOE) for the prediction of dense fog (surface visibility <200 m).

Time Window	Model	ACC	TPR	TNR	F1 Score
t-1	MCM	0.9743	0.7052	0.9794	0.9869
	ELM	0.9815	0.7133	0.9921	0.9871
	SVM	0.9888	0.6842	0.9945	0.9943
	MOE	0.9880	0.7387	0.9935	0.9939
t-2	MCM	0.9786	0.7052	0.9837	0.9891
	ELM	0.9888	0.6823	0.9900	0.9913
	SVM	0.9821	0.6842	0.9945	0.9943
	MOE	0.9824	0.4957	0.9938	0.9911
t-3	MCM	0.9790	0.8421	0.9815	0.9892
	ELM	0.9888	0.6842	0.9945	0.9943
	SVM	0.9813	0.3203	0.9946	0.9905
	MOE	0.9891	0.6844	0.9934	0.9965
t-4	MCM	0.9743	0.9157	0.9754	0.9868
	ELM	0.9803	0.0	1.0	0.9901
	SVM	0.9755	0.9200	0.9931	0.9838
	MOE	0.9888	0.6842	0.9945	0.9943
t-5	MCM	0.9605	0.8736	0.9621	0.9795
	ELM	0.9817	0.0	1.0	0.9908
	SVM	0.9817	0.0	1.0	0.9908
	MOE	0.9817	0.0	1.0	0.9908
t-1	Naive	0.9754	0.9982	0.9189	0.9873

in the case of fog for the previous period (t-1). The MOE and ELM attain optimal accuracy outcomes by incorporating supplementary variables during an extended time frame ranging from t-2 to t-5. Both of these options surpass the accuracy of the naive operator. The Naive operator's strong performance can be attributed to the imbalanced distribution of classes (fog / no fog or dense fog/no dense fog), as well as the limited number of low-visibility transitions (fog/no fog or dense fog/no dense fog). These findings suggest that the occurrence of low-visibility events at Patna airport is unusually long-lasting, but it is persistent for short periods. Therefore, the proposed MOE models outperform the benchmarked persistence-based and ML-based models and provide alternative and reliable ways of nowcasting low-visibility events for aviation services. Along with the earlier studies (Dutta and Chaudhuri, 2015; Shankar and Sahana, 2023a, 2023b), these studies can help choke out the mechanism that can directly sort out the crucial prediction of visibility for the aviation services in the local conditions of the IGP regions.

6. Conclusion

This study presents a noble analysis of the persistent nature of low-visibility events (fog (surface visibility <1000 m) and dense fog (surface visibility < 200 m) in a representative site (Patna Airport) of the fog-prone IGP regions of India by using the visibility time series as the objective variable. The study examined long-term and short-term persistence using the DFA and MCM methodologies, respectively. It indicates that dense fog occurrences are not persisting in nature for long periods but rather for short periods. The Markov chain probability transitions between fog and no-fog states, including dense fog and no-dense fog, have been utilized to examine short-term persistence analysis. These transitions have consistently demonstrated significant levels of persistence across all evaluated scenarios. Furthermore, conducting a detailed study to tap the potential of the persistence with the benchmark ML models to improve the prediction robustness of the low-visibility events (fog/no fog, or dense fog/no dense fog) in the specific conditions of the IGP regions for the practical application of the tailor-made now casting (lead time of 1 to 5 hours) of this extreme weather for the aviation services. Also conduct a detailed comparison of several ML models with the proposed Mixture of Experts (MOE), which taps the potential of persistence as well as hyper parameter-tuned machine learning models in the specific conditions of the IGP regions. ML-based models use external variables to consider conducive atmospheric conditions. The predictive skills of simplistic persistence models and their integration with machine learning approaches create a Mixture of Experts (MOE) to achieve precise prediction accuracy in the specific conditions of the IGP regions. The primary benefit of this tailor-made Nowcast for low-visibility events is that it generates output that applies to end users, such as air traffic managers, airlines, *etc*.

Data Availability

The hourly observed METAR data (or Synoptic hourly data) of weather parameters of JPNI Airport Patna was taken from the National Data Center, Climate Research Station of India Meteorological Department where weather data of India Meteorological Department is available through the portal https://dsp.imdpune.gov.in/. It is noted that this portal can be accessed publically. Also, data can be shared after the request.

Acknowledgements

The authors are thankful to the officials of the India Meteorological Department who are working on aviation and forecasting services, especially Ashish Kumar, Deepak Kumar Singh, and Uday Shankar Sinha, *etc*., for the useful discussion. AS is grateful to the Director General of Meteorology and the Third Vice President of WMO, Dr. M. Mohapatra, for their constant motivation.

Contributions

Conceptualization, A. S., B. C. S.; methodology, A. S.; software, A. S.; validation, A.S.; data curation, A.S.; writing-original draft preparation, A.S.; writing revised draft, A.S., B.C.S., S. P.S; supervision, B.C.S.; all authors have read and agreed to the published version of the manuscript.

Conflict of Interest

The authors declare no conflict of interest.

Funding

The author(s) assert(s) that no financial support, including funds, grants, or other forms of aid, was received for the development of this publication.

Disclaimer: The contents and views expressed in this research paper/article are the views of the authors and do not necessarily reflect the views of the organizations they belong to.

References

Bunde, A., Havlin, S., Kantelhardt, J. W., Penzel, T., Peter, J. H. and V. Karlheinz, 2000, "Correlated and uncorrelated regions in heart-rate fluctuations during sleep", *Phys. Rev. Lett.*, **85**, 17, 3608-3736.

Belo-Pereira, M. and Santos, J. A., 2016, "A persistent wintertime fog episode at Lisbon airport (Portugal): performance of ECMWF and AROME models", *Meteorological Applications*, **23**, 3, 353-370. doi : https://doi.org/10.1002/met.1560.

Boneh, T., Weymouth, G. T., Newham, P., Potts, R., Bally, J., Nicholson, A. E. and Korb, K. B., 2015, "Fog forecasting for Melbourne Airport using a Bayesian decision network", *Weather and Forecasting*, **30**, 5, 1218-1233. doi : https://doi.org /10.1175/WAF-D-15-0005.1.

Peng, C. K., Buldyrev, S. V., Havlin, S., Simons, M., Stanley, H. E., and A. L. G., 1994, "Mosaic organization of DNA nucleotides", *Phys. Rev. E*, **49**, 2, 1685.

Cazacioc, L., 2005, "Evaluation of the transition probabilities for daily precipitation time series using a Markov chain model", In *Proceedings of 3rd International Colloquium* (82-92). Bucharest, Romania. Retrieved from http://www. mathem.pub.ro/proc/bsgp-12/M-CAZ.PDF.

Chmielecki, R. M. and Raftery, A. E., 2011, "Probabilistic visibility forecasting using Bayesian model averaging. *Monthly Weather Review*, **139**, 5, 1626-1636. doi : https://doi.org/10.1175 /2010MWR3516.1.

Christopher, Chatfield., 1973, "Statistical Inference Regarding Markov Chain Models", *Applied Statistics*, **22**, 1, 7-20. doi : https://doi. org/https://doi.org/10.2307/2346299.

Cornejo-Bueno, L., Casanova-Mateo, C., Sanz-Justo, J., Cerro-Prada, E. and Salcedo-Sanz, S., 2017, "Efficient Prediction of Low-Visibility Events at Airports Using Machine-Learning Regression", *Boundary-Layer Meteorology*, **165**, 2, 349-370. doi : https://doi. org/10.1007/s10546-017-0276-8.

Cornejo-Bueno, S., Casillas-Pérez, D., Cornejo-Bueno, L., Chidean, M. I., Caamaño, A. J., Cerro-Prada, E. and Salcedo-Sanz, S., 2021, "Statistical analysis & machine learning prediction of fog-caused low-visibility events at a-8 motor-road in spain", *Atmosphere*, **12**, 6, doi: https://doi.org/10.3390/atmos12060679.

Cornejo-Bueno, S., Casillas-Pérez, D., Cornejo-Bueno, L., Chidean, M. I., Caamaño, A. J., Sanz-Justo, J. and Salcedo-Sanz, S., 2020, "Persistence analysis and prediction of low-visibility events at valladolid airport", Spain. *Symmetry*, **12**, 6, 1-18. doi : https:// doi.org/10.3390/sym12061045.

Cristianini, N. S. T., J., 2000, "An Introduction to Support Vector Machines and Other Kernel-Based Learning Methods", New York, NY, USA: Cambridge University Press.

Da Rocha, R. P., Gonçalves, F. L. T. and Segalin, B., 2015, "Fog events and local atmospheric features simulated by regional climate model for the metropolitan area of São Paulo, Brazil," *Atmospheric Research*, **151**, 176-188. doi : https://doi. org/10.1016/j.atmosres.2014.06.010.

Dhangar, N. G., Lal, D. M., Ghude, S. D., Kulkarni, R., Parde, A. N., Pithani, P. and Rajeevan, M., 2021, "On the Conditions for Onset and Development of Fog Over New Delhi: An Observational Study from the WiFEX", *Pure and Applied Geophysics*, **178**, 9, 3727-3746. doi : https://doi.org/10.1007/ s00024-021-02800-4.

Ding, S., Xu, X. and Nie, R., 2014, "Extreme learning machine and its applications. *Neural Computing and Applications*, **25** 3-4, 549–556. doi : https://doi.org/10.1007/s00521-013- 1522-8.

Dutta, D. and Chaudhuri, S., 2015, "Nowcasting visibility during wintertime fog over the airport of a metropolis of India: decision tree algorithm and artificial neural network approach", *Natural Hazards*, **75**, 2, 1349-1368. doi : https://doi.org/ 10.1007/s11069 -014-1388-9.

Fabbian, D., De Dear, R. and Lellyett, S., 2007, "Application of artificial neural network forecasts to predict fog at Canberra International Airport", *Weather and Forecasting*, **22**, 2, 372-381. doi : https:// doi.org/10.1175/WAF980.1.

Fawcett, T., 2006, "An introduction to ROC analysis", *Pattern Rec*, **27**, Lett., 861-874.

Fernández-González, S., Bolgiani, P., Fernández-Villares, J., González, P., García-Gil, A., Suárez, J. C. and Merino, A., 2019, "Forecasting of poor visibility episodes in the vicinity of Tenerife Norte Airport', *Atmospheric Research*, **223**, March, 49-59. doi : https://doi.org/10.1016/j.atmosres.2019.03.012.

Gadian, A., Dewsbury, J., Featherstone, F., Levermore, J., Morris, K. and Sanders, C., 2004, "Directional persistence of low wind speed observations. *Journal of Wind Engineering and Industrial Aerodynamics*, **92**, 12, 1061-1074. doi : https://doi.org/10.1016/ j.jweia.2004.05.007.

Graves, T., Gramacy, R., Watkins, N., Franzke, C., 2017, "A brief history of long memory: Hurst, Mandelbrot and the road to ARFIMA, 1951-1980", *Entropy*, **19**, 9, 1-21. doi : https://doi. org/10.3390/e19090437.

Guijo-Rubio, D., Gutiérrez, P. A., Casanova-Mateo, C., Sanz-Justo, J., Salcedo-Sanz, S., Hervás-Martínez, C., 2018, "Prediction of low-visibility events due to fog using ordinal classification", *Atmospheric Research*, **214**, July, 64-73. doi : https://doi.org /10.1016/j.atmosres.2018.07.017.

Gultepe, I., Tardif, R., Michaelides, S. C., Cermak, J., Bott, A., Bendix, J., and Cober, S. G., 2007, "Fog research: A review of past achievements and future perspectives", *Pure and Applied Geophysics*. doi : https://doi.org/10.1007/s00024-007-0211-x.

Fowler, H. J. S. B., and C. T., 2007, "Linking climate change modelling to impacts studies: recent advances in downscaling techniques for hydrological modelling", *International Journal of Climatology*, **27**, 1547-1578. https://doi.org/0.1002/joc.1556.

Haeffelin, M., Laffineur, Q., Bravo-Aranda, J. A., Drouin, M. A., Casquero-Vera, J. A., Dupont, J. C., De Backer, H., 2016, "Radiation fog formation alerts using attenuated backscatter power from automatic lidars and ceilometers", *Atmospheric Measurement Techniques*, **9**, 11, 5347-5365. doi : https://doi. org/10.5194/amt-9-5347-2016.

Herman, G. R. and Schumacher, R. S., 2016, "Using reforecasts to improve forecasting of fog and visibility for aviation", *Weather and Forecasting*, 31, 2, 467-482, doi: https://doi.org/10.1175 /WAF-D-15-0108.1.

Hosea, M. K., 2019, "Effect of Climate Change on Airline Flights Operations At Nnamdi Azikiwe International Airport Abuja, Nigeria", *Science World Journal*, **14**, 2, Retrieved from www.scienceworldjournal.org.

Hu, K., Ivanov, P. C., Chen, Z., Carpena, P. and Stanley, H. E., 2001, "Effect of trends on detrended fluctuation analysis", *Physical Review E - Statistical Physics, Plasmas, Fluids, and Related Interdisciplinary Topics*, **64**, 1, 19. doi : https://doi.org/10.1103/ PhysRevE.64.011114.

Huang, Guang Bin, Zhu, Q. Y., Siew, C. K., 2006, "Extreme learning machine: Theory and applications', *Neurocomputing*, **70**, 1-3, 489-501. doi : https://doi.org/10.1016/j.neucom.2005.12.126.

Huang, Gao, Huang, G. Bin, Song, S. and You, K., 2015, "Trends in extreme learning machines: A review", *Neural Networks*, **61**, 32-48. doi : https://doi.org/10.1016/j.neunet.2014.10.001.

IMD, Ministry of Earth Sciences, G., 2021, Standard Operation Procedure - Weather Forecasting and Warning Services Standard Operation Procedure Weather Forecasting and Warning.

Kantelhardt, J. W., Koscielny-Bunde, E., Rego, H. A., Havlin S. and A. B., 2001, "Detecting long-range correlations with detrended fluctuation analysis", *Physica A*, **295**, 3, 2001, 441-454.

Jiang, L., 2018, "Mean wind speed persistence over China", *Physica A: Statistical Mechanics and Its Applications*, **502**, 211-217. doi : https://doi.org/10.1016/j.physa.2018.02.058.

Katz, R. W., 1977, "Precipitation as a Chain-Dependent Process", *J. Appl. Met*, **16**, 671-676.

Koçak, K., 2008, "Practical ways of evaluating wind speed persistence. *Energy*, **33**, 1, 65-70. https://doi.org/10.1016/j.energy. 2007.07. 010.

Kohavi, R., 1995, "A study of cross-validation and bootstrap for accuracy estimation and model selection", *Int. Jt. Conf. Artif. Intell*, **14**, 1137-1145.

Koyuncu, R., Deniz, A. and Özdemir, E. T., 2022, "Ankara Esenboga International Airport (Turkey) fog analysis and synoptical investigation of the fog event dated 17–19 December 2019", *International Journal of Climatology*, **42**, 16, 8368-8389. doi : https://doi.org/10.1002/joc.7728.

Koziara, M., Robert, J., Thompson, W., 1983, "Estimating Marine Fog Probability Using a Model Output Statistics Scheme", *Monthly Weather Review*, 111, 12, 2333-2340. https://doi.org/10.1175/1520-0493(1983)111<2333:EMFPUA>2.0.CO;2.

Kulkarni, R., Jenamani, R. K., Pithani, P., Konwar, M., Nigam, N. and Ghude, S. D., 2019, "Loss to aviation economy due to winter fog in New Delhi during the winter of 2011-2016", *Atmosphere*, **10**, 4, 1-10. doi : https://doi.org/10.3390/ATMOS10040198.

Kutty, S. G., Agnihotri, G., Dimri, A. P. and Gultepe, I., 2019, "Fog Occurrence and Associated Meteorological Factors Over Kempegowda International Airport, India. *Pure and Applied Geophysics*, **176**, 5, 2179-2190. doi : https://doi.org/10.1007/s00024-018-1882-1.

Jiang, L., Li, N. and X. Z., 2017, "Scaling behaviors of precipitation over China", *Theor. Appl. Climatol.*, **128**, 1-2, 63-70.

Lakra, K. and Avishek, K., 2022, "A review on factors influencing fog formation, classification, forecasting, detection and impacts" *Rendiconti Lincei*, **33**, Springer International Publishing. doi : https://doi.org/10.1007/s12210-022-01060-1.

Lo, W. L., Zhu, M. and Fu, H., 2020, "Meteorology visibility estimation by using multi-support vector regression method", *Journal of Advances in Information Technology*, **11**, 2, 40-47. doi : https://doi.org/10.12720/jait.11.2.40-47.

Luo, M., Leung, Y., Zhou Y. and W. Z., 2015, "Scaling Behaviors of Global Sea Surface Temp.", *J. Climate*, **28**, 8, 3122-3132.

Mann, M. E., 2011, "On long range dependence in global surface temperature series. *Climatic Change"*, **107**, 3, 267-276. doi : https://doi.org/10.1007/s10584-010-9998-z.

Miao, K. chao, Han, T. ting, Yao, Y. qing, Lu, H., Chen, P., Wang, B. and Zhang, J., 2020, "Application of LSTM for short term fog forecasting based on meteorological elements", *Neurocomputing*, **408**, 285-291. doi : https://doi.org/10.1016/j.neucom.2019.12.129

Miao, Y., Potts, R., Huang, X., Elliott, G. and Rivett, R., 2012, "A fuzzy logic fog forecasting model for Perth Airport. *Pure and Applied Geophysics*, **169** 5-6, 1107-1119. doi : https://doi.org/10.1007/s00024-011-0351-x.

Mohan, K. N., Paligan, A. A., Sivakumar, G., Krishnamurthy, R., Shubha, V., Shinde, U. and Bhatnagar, M. K., 2015, "Performance study of Drishti transmissometer at CAT III B airport", *MAUSAM*, **66**.

Müller, M. D., Masbou, M. and Bott, A., 2010, "Three-dimensional fog forecasting in complex terrain", *Quarterly Journal of the Royal Meteorological Society*, **136**, 653, 2189-2202. doi : https://doi.org/10.1002/qj.705.

Niu, S., Lu, C., Yu, H., Zhao, L. and Lü, J., 2010, "Fog research in China: An overview", *Advances in Atmospheric Sciences*, **27**, 3, 639-662. https://doi.org/10.1007/s00376-009-8174-8.

P. Talkner, and R. O. W., 2000, "Power spectrum and detrended fluctuation analysis: application to daily temperatures", *Phys. Rev. E*, **62**, 1, 150.

Pahlavan, R., Moradi, M., Tajbakhsh, S., Azadi, M., Rahnama, M., 2021, "Fog probabilistic forecasting using an ensemble prediction system at six airports in Iran for 10 fog events", *Meteorological Applications*, **28**, 6, 1-16. doi : https://doi.org/10.1002/met.2033.

Parde, A. N., Ghude, S. D., Dhangar, N. G., Lonkar, P., Wagh, S., Govardhan, G. and Jenamani, R. K., 2022, "Operational Probabilistic Fog Prediction Based on Ensemble Forecast System: A Decision Support System for Fog. *Atmosphere*, **13**, 10, 1-17. doi : https://doi.org/10.3390/atmos13101608.

Pelletier, J. D., Turcotte, D. L., 1997, "Long-range persistence in climatological and hydrological time series: Analysis, modeling and application to drought hazard assessment", *Journal of Hydrology*, **203**, 1-4, 198-208. doi : https://doi.org/10.1016/S0022-1694(97)00102-9.

Pérez-Ortiz, M., Gutiérrez, P. A., Tino, P., Casanova-Mateo, C. and Salcedo-Sanz, S., 2018, "A mixture of experts model for predicting persistent weather patterns", *Proceedings of the International Joint Conference on Neural Networks*, *2018-July*. doi : https://doi.org/10.1109/IJCNN.2018.8489179.

María, Pérez-Ortiz, Jiménez-Fernández, S., Gutiérrez, P. A., Alexandre, E., Hervás-Martínez, C. and Salcedo-Sanz, S., 2016, "A review of classification problems and algorithms in renewable energy applications", *Energies*, **9**, 8, 1-27. doi : https://doi.org/10.3390/en9080607

Pithani, P., Ghude, S. D., Chennu, V. N., Kulkarni, R. G., Steeneveld, G. J., Sharma, A. and Madhavan, R., 2019, "WRF Model Prediction of a Dense Fog Event Occurred During the Winter Fog Experiment (WIFEX)", *Pure and Applied Geophysics*, **176**, 4, 1827-1846. doi : https://doi.org/10.1007/s00024-018-2053-0.

Price, J., Porson, A., Lock, A., 2015, "An Observational Case Study of Persistent Fog and Comparison with an Ensemble Forecast Model", *Boundary-Layer Meteorology*, **155**, 2, 301-327. doi : https://doi.org/10.1007/s10546-014-9995-2.

Blender, R., K. F., 2003, "Long time memory in global warming simulations", *Geophys. Res. Lett.*, **30**, 14, 1769.

Monetti, R. A., Havlin S, A. B., 2003, "Long term persistence in the sea-surface temperature fluctuations", *Physica A*, **320**, 581-589.

Govindan, R. B., D. Vyushin, A. Bunde, S. Brenner and S. Havlin, H. J. S., 2002, "Global climate models violate scaling of the observed atmospheric variability", *Phys. Rev. Lett.*, **89**, 028501.

Román-Cascón, C., Steeneveld, G. J., Yagüe, C., Sastre, M., Arrillaga, J. A., Maqueda, G., 2016, "Forecasting radiation fog at climatologically contrasting sites: Evaluation of statistical methods and WRF", *Quarterly Journal of the Royal Meteorological Society*, **142**, 695, 1048-1063. doi : https://doi.org/10.1002/qj.2708.

Román-Cascón, C., Yagüe, C., Sastre, M., Maqueda, G., Salamanca, F. and Viana, S., 2012, "Observations and WRF simulations of fog events at the Spanish Northern Plateau", *Advances in Science and Research*, **8**, 1, 11-18. doi : https://doi.org/10.5194/asr-8-11-2012.

Román-Cascón, Carlos, Yagüe, C., Steeneveld, G. J., Morales, G., Arrillaga, J. A., Sastre, M. and Maqueda, G., 2019, "Radiation and cloud-base lowering fog events: Observational analysis and evaluation of WRF and HARMONIE", *Atmospheric Research*, **229**, 190-207. https://doi.org/10.1016/j.atmosres.2019.06.018.

Salcedo-Sanz, S., Piles, M., Cuadra, L., Casanova-Mateo, C., Caamaño, A. J., Cerro-Prada, E. and Camps-Valls, G., 2021a, "Long-term persistence, invariant time scales and on-off intermittency of fog events", *Atmospheric Research*, **252**, (November 2020). doi : https://doi.org/10.1016/j.atmosres.2021.105456.

Salcedo-Sanz, S., Piles, M., Cuadra, L., Casanova-Mateo, C., Caamaño, A. J., Cerro-Prada, E. and Camps-Valls, G., 2021b, "Long-term persistence, invariant time scales and on-off intermittency of fog events", *Atmospheric Research*, **252**, September 2020, doi : https://doi.org/10.1016/j.atmosres.2021.105456.

Salcedo-Sanz, S., Rojo-Álvarez, J. L., Martínez-Ramón, M. and Camps-Valls, G., 2014, "Support vector machines in engineering: An overview", *Wiley Interdisciplinary Reviews: Data Mining and Knowledge Discovery*, **4**, 3, 234-267. doi : https://doi.org/10.1002/widm.1125.

Sasaki, Y., 2007, "The truth of the F-measure" *Teach Tutor Mater*, *1*, 1-5.

Sawaisarje, G. K., Khare, P., Shirke, C. Y., Deepakumar, S., Narkhede, N. M., 2014, "Study of winter fog over Indian subcontinent: Climatological perspectives", *MAUSAM*, **65**, 1, 19-28. doi : https://doi.org/10.54302/mausam.v65i1.858.

Schölkopf, B. and Smola, A., 2002, "Learning with Kernels-Support Vector Machines, Regularization", *Optimization and Beyond*. Cambridge, MA, USA: MIT Press.

Shankar, A. and Giri, R. K., 2024, "The Impacts of Low Visibility on the Aviation Services of Patna Airport During the Period from 2016 to 2023", *Journal of Airline Operations and Aviation Management*, doi : https://doi.org/10.56801/jaoam.v3i1.53(1).

Shankar, A., Kumar, A., Sahana, B. C. and Sinha, V., 2022, "A Case Study of Heavy Rainfall Events and Resultant Flooding During the Summer Monsoon Season 2020 Over the River Catchments of North Bihar, India", *Vayumandal*. **48** (August 2008), 17-28.

Shankar, A. and Sahana, B. C., 2023a, "Early warning of low visibility using the ensembling of machine learning approaches for aviation services at Jay Prakash Narayan International (JPNI) Airport Patna", *SN Applied Sciences*. doi : https://doi.org/10.1007/s42452-023-05350-7.

Shankar, A. and Sahana, B. C., 2023b, "Efficient prediction of runway visual range by using a hybrid CNN-LSTM network architecture for aviation services", *Theoretical and Applied Climatology*, (Icao 2010). doi : https://doi.org/10.1007/s00704-023-04751-3.

Singh, A., George, J. P. and Iyengar, G. R., 2018, "Prediction of fog/visibility over India using NWP Model", *Journal of Earth System Science*, **127**, 2, 1-13. doi : https://doi.org/10.1007/s12040-018-0927-2.

Singh J. and Kant S., 2006, "Radiation fog over north India during winter from 1989-2004", *Mausam*, **57**, April, 271-290.

Smith, D. K.E., Renfrew, I. A., Price, J. D. and Dorling, S. R., 2018, "Numerical modelling of the evolution of the boundary layer during a radiation fog event. *Weather*, **73**, 10, 310-316. doi : https://doi.org/10.1002/wea.3305.

Smith, Daniel K. E., Dorling, S. R., Renfrew, I. A., Ross, A. N. and Poku, C., 2023, "Fog trends in India: Relationships to fog type and western disturbances. *International Journal of Climatology*, **43**, 2, 818-836. doi : https://doi.org/10.1002/joc.7832

Stolaki, S. N., Kazadzis, S. A., Foris, D. V. and Karacostas, T. S., 2009, "Fog characteristics at the airport of Thessaloniki, Greece", *Natural Hazards and Earth System Science*, **9**, 5, 1541-1549. doi : https://doi.org/10.5194/nhess-9-1541-2009

Sumathi, S., Paneerselvam, S., 2020, "Computational Intelligence. Computational Intelligence Paradigms, 25-52. doi : https://doi.org/10.1201/9781439809037-6.

Van, Der, Velde, I. R., Steeneveld, G. J., Wichers Schreur, B. G. J., Holtslag and A. A. M., 2010, "Modeling and forecasting the onset.and duration of severe radiation fog under frost conditions, *Monthly Weather Review*, **138**, 11, 4237-4253. doi : https://doi.org/10.1175/2010MWR3427.1

Voyant, C., Notton, G., 2018, "Solar irradiation nowcasting by stochastic persistence: A new parsimonious, simple and efficient forecasting tool", *Renewable and Sustainable Energy Reviews*, **92** (October 2017), 343-352. doi : https://doi.org/10.1016/j.rser.2018.04.116.

Wilks, D. S., 2011, "*Statistical Methods in the Atmospheric Sciences*", Cambridge, MA, USA: Academic Press.

World Meteorological Organization, 2019, *Manual on Codes International Codes* (2019 editi). WMO-No. 306 © World Meteorological Organization, 2019.

X. Chen, G.X. Lin and Z. T. F., 2007, "Long-range correlations in daily relative humidity fluctuations: A new index to characterize the climate regions over China", *Geophys. Res. Lett.*, **34**, 7, L07804.

Yang, L. and Fu, Z., 2019, "Process-dependent persistence in precipitation records", *Physica A: Statistical Mechanics and Its Applications*, **527**, 121459. doi : https://doi.org/10.1016/j.physa. 2019.121459.

Zhang, W. F. and Zhao, Q., 2015, "Asymmetric long-term persistence analysis in sea surface temperature anomaly", *Physica A: Statistical Mechanics and Its Applications*, **428**, 314-318. doi : https://doi.org/10.1016/j.physa.2015.01.081.

This manuscript employs the following abbreviations:

DFA	Detrended Fluctuation Analysis	TN	True Negative
WMO	World Meteorological Organization	TP	True Positive
ML	Machine Learning	FP	False Positive
MCM	Markov Chain Model	FN	False Negative
MOE	Mixture of Expert	P	Number of Real Positive
SVM	Support Vector Machine	N	Number of Real Negative
TPR	True Positive Rate	JPNI Airport	Jay Prakash Narayan International Airport
TNR	True Negative Rate	IGP	Indo Gangetic Plain
TP	True Positive	NWP	Numerical Weather Prediction
ELM	Extreme Learning Machine	ATM	Air Traffic Management